Pertanika J. Sci. & Technol. 34 (S2): 37 - 50 (2026)

PERTANIKA JOURNALS

SCIENCE & TECHNOLOGY

Journal homepage: http://www.pertanika.upm.edu.my/

Correlation Between Compressive and Flexural Properties in Steel Fibre Reinforced Concrete (SFRC) Beam Using Regression Analysis

Md Yushairi Kamarul Effendy Mohd Yusof[1], Anizahyati Alisibramulisi[2,3]*, Muhd Norhasri Muhd Sidek[2,3], Nadiah Saari[2], and Suraya Hani Adnan[4]

[1]ARUP Jururunding Sdn. Bhd., Level 26, 1 Powerhouse, No. 1 Persiaran Bandar Utama, Bandar Utama, 47800 Petaling Jaya, Selangor, Malaysia

[2]Faculty of Civil Engineering, Universiti Teknologi MARA, 40450 Shah Alam, Selangor, Malaysia

[3]Institute for Infrastructure Engineering and Sustainable Management (IIESM), Universiti Teknologi MARA, 40450 Shah Alam, Selangor, Malaysia

[4]Department of Civil Engineering Technology, Faculty of Engineering Technology, Universiti Tun Hussein Onn Malaysia, 84600 Pagoh, Johor, Malaysia

ABSTRACT

This study evaluated Ground-Penetrating Radar (GPR) to assess steel fibre distribution in Steel Fibre Reinforced Concrete (SFRC) beams and correlated non-destructive and mechanical strength properties. High-Performance Concrete (C60) beam specimens (100 mm × 100 mm × 500 mm) were prepared with steel fibre volume fractions of 0.5%, 1.0%, and 1.5%. Non-destructive testing (GPR, Rebound Hammer) and destructive testing (3000 kN compressive and 1000 kN flexural strength) were conducted at 7, 21, and 28 days. GPR radargrams displayed hazy patterns with overlapping hyperbolas, confirming uniform fibre distribution. Haze intensity increased at 1.5% fibre content. Compressive strength peaked at a 0.5% fibre fraction, whereas flexural strength reached its optimum at 1.5%. Linear Regression Analysis (NCSS 2021) demonstrated a strong R2 fit between compressive and flexural strengths. Overall, GPR proves effective for non-destructive fibre evaluation, aiding quality assessment in high-performance concrete structures.

Keywords: Compressive, flexural, Ground Penetrating Radar (GPR), regression analysis, Steel Fibre Reinforced Concrete (SFRC)

ARTICLE INFO

Article history:
Received: 18 June 2026
Accepted: 19 August 2026
Published: 30 September 2026

DOI: https://doi.org/10.47836/pjst.34.S2.04

E-mail addresses:
mdyushairi@gmail.com (Md Yushairi Kamarul Effendy Mohd Yusof)
aniza659@uitm.edu.my (Anizahyati Alisibramulisi)
muhdnorhasri@uitm.edu.my (Muhd Norhasri Muhd Sidek)
nadiahsaari@uitm.edu.my (Nadiah Saari)
suraya@uthm.edu.my (Suraya Hani Adnan)
* Corresponding author

INTRODUCTION

Steel Fibre Reinforced Concrete (SFRC) is a structural reinforcing technology that aims to reduce the demand for reinforcement while simultaneously increasing the flexural toughness, flexural strength,

e-ISSN: 2231-8526

© Universiti Putra Malaysia Press

fatigue resistance, impact resistance, and post-fracture strength of the concrete. The Non-Destructive Testing (NDT) method has been used to investigate a variety of concrete issues. Although SFRC beams may exhibit higher compressive and flexural strength, there is a dearth of research on the use of Ground-Penetrating Radar (GPR) to analyse concrete quality in relation to SFRC beam strength, compared with conventional reinforced concrete. Additionally, there is a dearth of studies about the uniformity of steel fibres in SFRC beams. It is observed that most published empirical relationships have been reported for conventional concrete and SFRC; however, few have been studied for SFRC using regression and Pearson correlation analyses.

Bibliometric studies are defined as statistical evaluations and tools used to achieve quantitative research of published journal papers, proceedings, scholars, scientific articles or books, and are an effective method to assess the influence of journal papers, authors' research areas, citation networks, topics, and documents (Briones-Bitar et al., 2020; Van Eck & Waltman, 2020). VOSviewer software was used to construct and visualise the bibliometric networks of journal papers related to GPR.

GPR is a non-destructive testing technique that uses a scanning method and is currently in wide use in the civil engineering field, with a potential application in concrete testing (Dinh et al., 2013; Giannopoulos, 2005; Lakshmi et al., 2016; Sultan et al., 2020; Warren & Giannopoulos, 2016).

According to early research by Bachiri et al. (2018), Morcous and Erdogmus (2009), and Sun et al. (2018), the GPR method achieves 98%- 99% accuracy in detecting rebar position, delamination, and corrosion defects. Lakshmi et al. (2016), Leucci (2012), Rathod et al. (2019), and He et al. (2009) have demonstrated in their studies that the difference in rebar radius estimates is about 2.5% to 6% when using the GPR method on bridge decks and reinforced concrete slabs. The use of GPR in reinforced concrete can detect concrete delamination and rebar corrosion at an early stage (Shamsudin et al., 2015; Sun et al., 2018; Zaki et al., 2018) and assess the thickness of concrete pavement (Morcous & Erdogmus, 2009). Other researchers have used the GPR technique to detect air void size and depth (Razak et al., 2015) and to estimate the volumetric water content in reinforced concrete (Leucci, 2012).

For steel fibre fractions of 0%, 0.5%, 1.0%, and 1.5%, there is a marginal improvement in compressive strength from 0.5% to 1.0%, followed by a decrease from 1.0% to 1.5%. The compressive strength increased with increasing steel fibre volume fraction from 0% to 3.0%, reaching a maximum at 3.0%. Findings from Al-Ameeri (2013) indicate that compressive strength increases with age and with the steel fibre volume fraction up to 0.75% and decreases when the steel fibre volume fraction exceeds 0.75%. As the steel fibre volume fraction increases from 0% to 3.0%, the compressive strength of concrete increases progressively owing to the balling effect, and inappropriate bonding occurs

beyond 3.0% (Al-Ameeri, 2013). Harle (2019) discovered that the optimal steel fibre content for compressive cube strength is 1.0%.

Increasing the steel fibre volume fraction from 0% to 3.0% was found to increase flexural strength and improve resistance to cracking (Kumar Athithan et al., 2017). According to Al-Ameeri (2013), flexural strength increases continuously with increasing steel fibre volume fraction up to 1.5%. According to studies conducted by Al-Ameeri (2013), the addition of steel fibre to concrete increases the flexural strength continuously as the steel fibre fraction volume increases from 0% to 3.0%, but as the steel fibre fraction volume increases above 3.0%, the flexural strength appears to decrease gradually due to the balling effect and improper bonding with the concrete.

Incorporating steel fibres reduces the workability of new concrete and increases the likelihood of non-uniform dispersion. The water-cement ratio may be increased, or water-reducing admixtures may be used. According to Eurocode 2, steel fibres don't change the tensile strength of the concrete itself. They can, however, reduce cracking and help concrete parts be more ductile (Al-Ameeri, 2013; Jhatial et al., 2018; Neville, 2012; Shetty, 2012).

In this study, the correlation between compressive strength and flexural strength was explored using Linear Regression Analysis and Pearson Correlation. Correlation analysis quantifies the degree and direction of the linear relationship between two variables, while basic linear regression estimates parameters in a linear equation that can be used to forecast one variable from the other (Profillidis & Botzoris, 2019). A total of 878 authors, with a minimum of 5 documents per author, are repeated in the publication and conduct studies related to ground-penetrating radar. Only 17 authors with publications in ground penetrating radar meet the threshold. The total strength of the co-authorship links with other authors was calculated by Vos viewer, and the greatest total link strength was selected. In total, the 17 authors who conducted studies on the application of ground-penetrating radar to existing structures can be clustered into 9 groups, indicating a strong bond among them, as shown in Figure 1.

There was a total of 24 authors, each of whom has at least one paper related to the publication, who undertake research on ground-penetrating radar and steel fibre-reinforced concrete. The 24 authors with publications on ground-penetrating radar in steel fibre-reinforced concrete that meet the threshold. Figure 2 shows that the 24 authors have strong bond links and co-occurrence in studies on the application of GPR to steel fibre-reinforced concrete, with eight clusters of co-authorship that are linked to each other. Some of the 24 authors in the network are not connected to each other (Van Eck & Waltman, 2020). Based on the schematic literature, GPR is most widely used on existing concrete structures and is also used abroad.

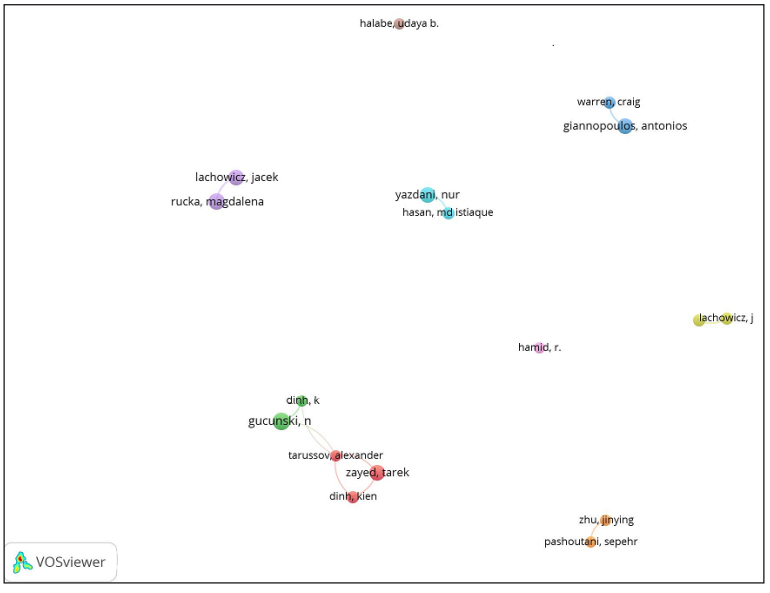

Figure 1. Authors are grouped into 9 clusters, as reported in GPR studies



Figure 2. A total of 24 authors linked studies on GPR applications to steel fibre-reinforced concret

METHODOLOGY

A comprehensive method and methodology will aid in understanding the underlying principle and the experimental procedure. This research methodology describes the experimental setup, test procedures for non-destructive and destructive tests, linear

regression analysis, and Pearson correlation for conducting the test regime undertaken in the present research topic. Data collection for this experimental study shall be collected by using GPR equipment IDS GeoRadar TR-HF with antenna 2.0 GHz, Rebound Hammer Test and Flexural Test for scanning and testing the specimen sample SFRC beam and RC beam prepared in laboratory environment condition and field test data of GPR, Rebound Hammer Test, Flexural Test and Cube Compressive Test/Broken Beam Compressive Test to specimen sample SFRC beam and RC beam shall be process for evaluation, analysis and modelled in linear regression analysis using NCSS 2021 software (Hintze, 2007). The experimental work that will be used in this study is to determine the application and effectiveness of the GPR application and to study the strength of SFRC using GPR, with a correlation of the Rebound Hammer Test and the behaviour of the SFRC beam using the Flexural Test Method from the experimental work, as shown in Figure 3.

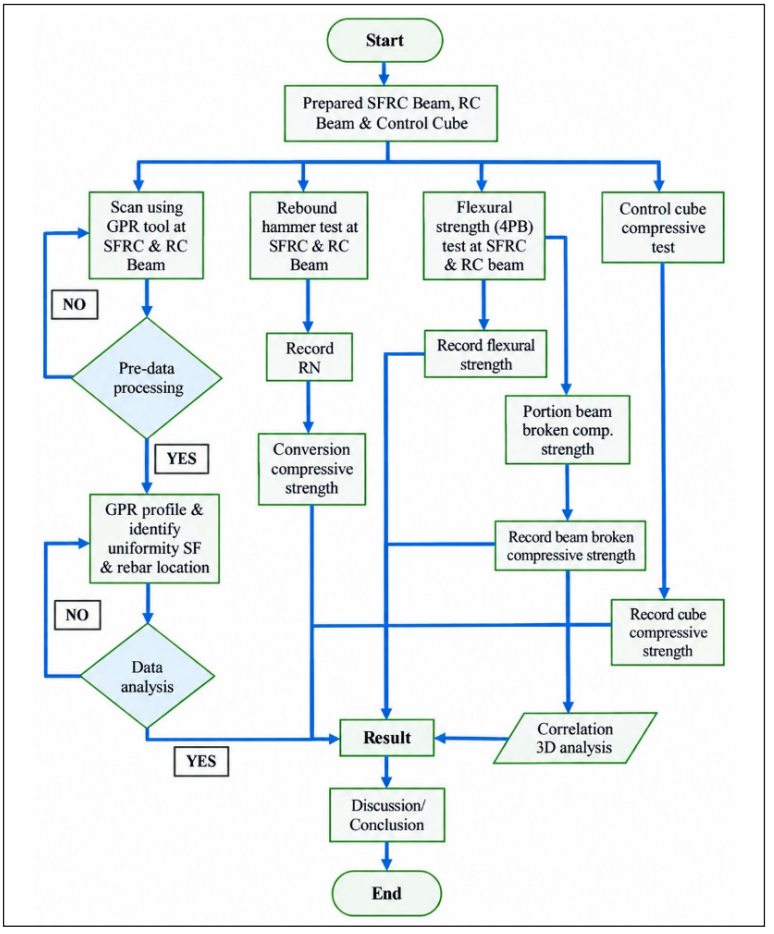

Figure 3. Methodology in this study

RESULTS AND DISCUSSION

GPR - Radargram

Figure 4a shows the radargram B-scan image section of the reinforced concrete beam control sample in X-plane and Y-plane, where the target formed a hyperbolic shape to represent the reinforcement bar detected embedded in the control samples. This finding is in line with other researchers' (Gehrig, 2004; Hasan & Yazdani, 2016; Jaya, 2013; Lakshmi et al., 2016; Leucci, 2012; Liu et al., 2020; Rathod et al., 2019; Wiwatrojanagul et al., 2018; Zhou et al., 2018) efforts to identify the location and reinforcement bar diameter. Figure 4b shows the radargram B-scan image section of the SFRC beam sample with a different steel fibre fraction volume. It can be observed that for the steel fibre mix, the radargram does not show the expected result of the hyperbola shape found in the RC beam (Maierhofer, 2003); instead, the radargram image shows a hazy image like a radio static wave and multiply hyperbola with overlapping each other, with no distinct apparent reflection of individual hyperbolas as embedded reinforcement bars. This shows the uniformity of steel fibre in the SFRC beam. The radargram image for the SFRC beam, under hazy conditions, has become heavier and more sophisticated as the steel fibre volume fraction increased from 0.5% to 1.5%.

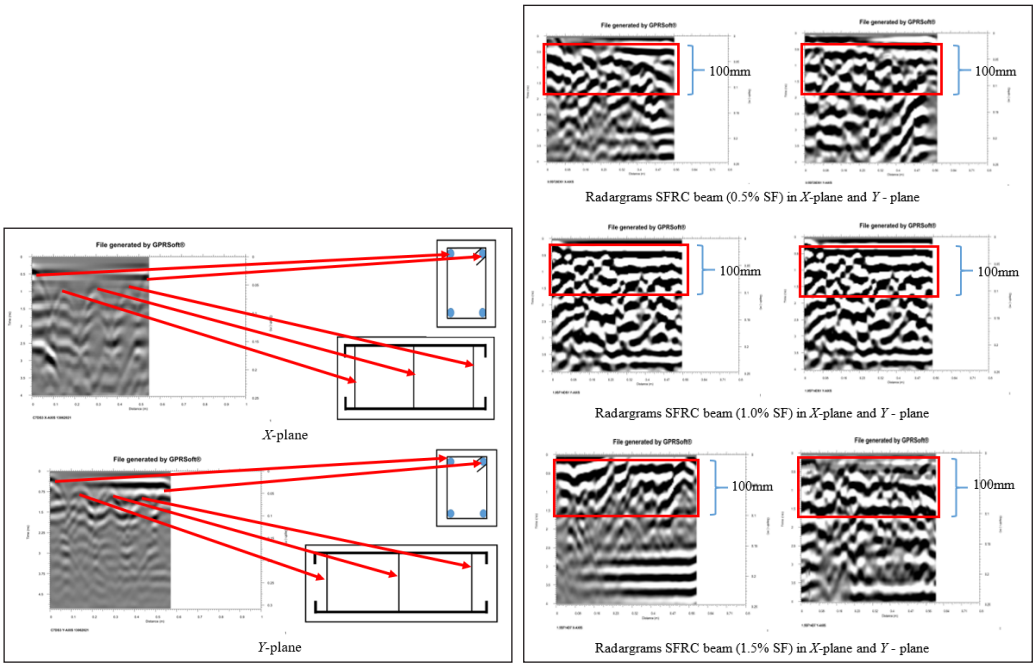

Figure 4. Tabulation of (a) Radargrams RC beam size 100mm × 100mm × 500mm in X-plan and Y-plane (b) Radargrams SFRC beam (0.5%, 1.0%, and 1.5% steel fibre) in X-plane and Y-plane

Compressive and Flexural Strength

From Figure 5, the cube compressive strength test result, it is shown that the addition of steel fibres in the concrete helps to increase the concrete strength when 0.5% steel fibre and 1.5% steel fibre fraction volume are added to the concrete, given the compressive values of 181.2 N/mm^2 and 88.1 N/mm^2 at 28 days of concrete age. When a 1.0% steel fibre volume fraction is added to the concrete, the concrete's compressive strength decreases from 139.5 N/mm^2 at 7 days to 98.2 N/mm^2 at 28 days of ageing. Based on the cube compressive strength test result at 28 days of concrete age, the optimum fibre content for SFRC was found to be 0.5% steel fibre, given a compressive strength of 181.2 N/mm^2. The finding on the optimum steel fibre content for compressive strength is in line with studies by Al-Ameeri (2013) and Rao (2010), which found that steel fibre contents of 0.5% to 1.0%, 0.75%, and up to 3.0% increase the compressive strength of SFRC. Similar findings from studies by Rao (2010) and Al-Ameeri (2013) for 1.0% steel fibre content show a decrease in compressive strength.

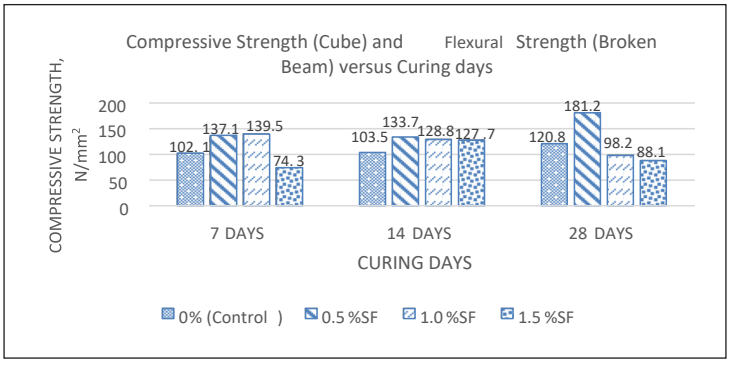

Figure 5. Compressive strength (cube) and flexural strength (broken beam) versus curing days

Figure 6, representing 3 different case studies with loading spans of 102.3 mm, 136.4 mm, or 181.8 mm, shows that the control sample with a reinforcement bar has the best flexural strength compared to those with steel fibre added as an alternative. In comparison to an SFRC with a different volume fraction, the SFRC exhibits an increase in flexural strength as the volume fraction of steel fibre increases. Based on three distinct case studies with loading spans of 102.3mm, 136.4mm, and 181.8mm, a 1.5% steel fibre volume fraction exhibits the highest flexural strength on day 28 compared with other SFRC samples, whereas a 0.5% steel fibre volume fraction exhibits the lowest. The results indicate that a 1.5% steel fibre volume fraction in SFRC yields the highest flexural strength, followed by 0.5% and 1.0%. This finding is in line with studies by Al-Ameeri (2013) and Kumar Athithan et al. (2017). The control sample with a reinforcement bar is much stronger than the steel fibre sample in terms of flexural strength.

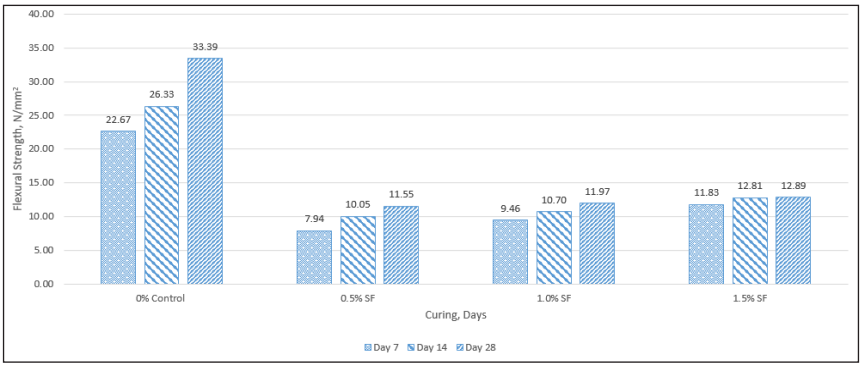

(a)

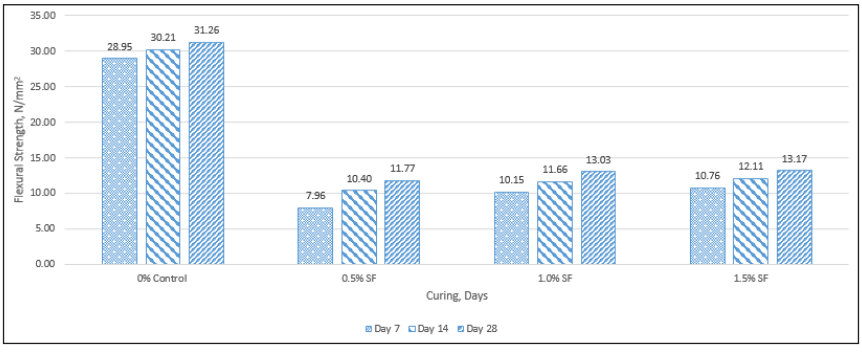

(b)

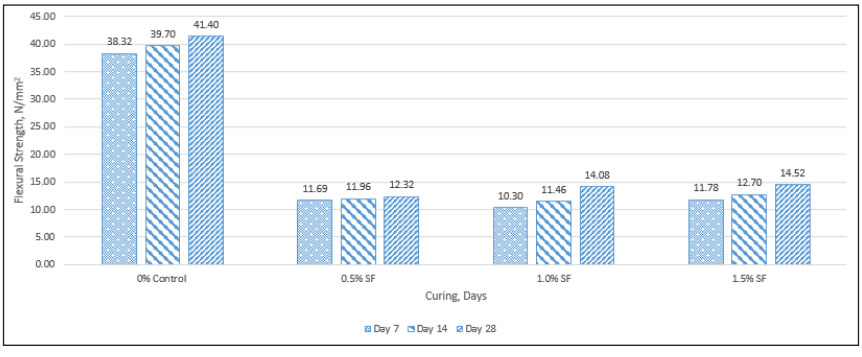

(c)

Figure 6. Tabulation of flexural strength (N/mm^2) with respect to curing days (a) Case 1; (b) Case 2; (c) Case 3

Using the collected experimental dataset, the correlation between steel fibre and the compressive and flexural strengths of SFRC beams has been assessed by performing Linear Regression Analysis and Pearson Correlation. The empirical or correlation equation model obtained for the compressive strength of cubes and beams broken for SFRC beams is presented in Equation 1:

$$fck\ cube\ comp\ BB\ cube = (129.3083) + (-12.9567)Vf \quad [1]$$

Where,
fck cube comp BB cube = Cube and beams broken compressive strength (N/mm^2),
Vf = steel fibre volume fraction.

The empirical or correlation equation model obtained for flexural strength for SFRC beam are pre-sented in Equation 2:

$$flexural\ strength,\ \sigma = (24.5684) + (-11.2783)\ Vf \quad [2]$$

Where,
flexural strength, σ = Flexural strength (N/mm^2),
Vf = steel fibre volume fraction.

The empirical or correlation equation model obtained for compressive strength conversion of rebound number (RN) for SFRC beams is presented in Equation (3):

$$fck\ cube\ comp\ RN = (37.1307) + (-0.0387)Vf \quad [3]$$

Where,
fck cube comp RN = RN conversion compressive strength (N/mm^2),
Vf = steel fibre volume fraction.

Figure 7 shows the test values for compressive strength, flexural strength, and steel fibres, based on a linear regression model. It can be seen from Fig. 7a and 7b that the concrete compressive cube beams broken test and flexural strength test have a moderate correlation with the steel fibre values. This shows that the steel fibre volume fraction has had a significant effect on the concrete during preparation, resulting in both high and low strength. Compared with the concrete compressive strength conversion from rebound number (RN) in Fig. 7c, the result shows a very weak correlation with the steel fibre values. This may be due to inconsistent rebound hammer test results and handling errors during testing.

The results of the linear regression analysis between the test value and the predicted value of SFRC strength are shown in Table 1. As shown in Table 1, a significance test for the slope indicates that the compressive strength of the cube beams and steel fibres is zero, resulting in a t-value of -1.6072. The significance level of this t-test was 0.1173. Since 0.1173 > 0.0500, the hypothesis that the slope is zero is not rejected.

The estimated slope was -12.9567, and the intercept was 129.3083. The lower limit of the 95% confidence interval for the intercept was 113.9834, and the upper limit was 144.6333.

Besides, a significance test for the slope represents flexural strength, and the steel fibre is zero, resulting in a t-value of -5.5115. The significance level of this t-test was 0.1063. Since 0.1063 > 0.0500, the hypothesis that the slope is zero is not rejected. The estimated slope was -11.2783, and the intercept was 24.5684. The lower limit of the 95% confidence interval for the intercept was 20.6784, and the upper limit was 28.4585. In addition, a significance test for the slope indicates that the compressive strength of the rebound number (RN) conversion and steel fibre is significant, resulting in a t-value of 0.0289. The significance level of this t-test was 0.9771. Since 0.9771 > 0.0500, the hypothesis that the slope is zero is not rejected. The estimated slope was -0.0387, and the intercept was 37.1307. The lower limit of the 95% confidence interval for the intercept was 34.5842, and the upper limit was 39.6771.

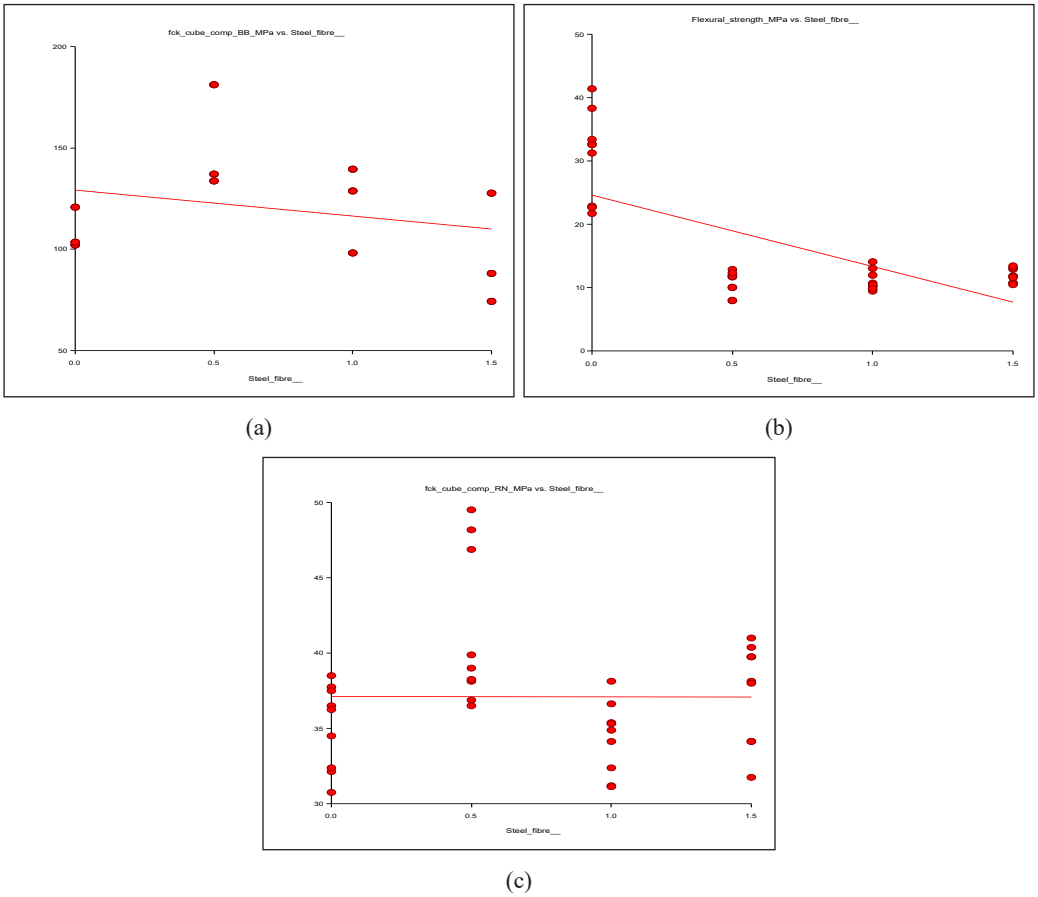

(a) (b)

(c)

Figure 7. Tabulation of test values of the compressive-flexural strength and steel fibre (a) compressive cube beams broken strength; (b) flexural strength; (c) compressive cube RN

Table 1
Result of linear regression-based analysis between test values and predicted values of SFRC strength

	Slope	Intercept	Lower Limit of 95% Confidence Interval (C.I)	Upper Limit of 95% Confidence Interval (C.I)	t-value	Significance Level of t-test	ANOVA	
							Sum of Squares	F-Ratio
Compressive Strength Cube & Beams	-12.9567	129.3083	113.9834	144.6333	-1.6072	0.1173	514870.8	2.5831
Flexural Strength	-11.2783	24.5684	20.6784	28.4585	-5.5115	0.1063	9342.8	30.3762
Compressive Strength RN	-0.0387	37.1307	34.5842	39.6771	-0.0289	0.9771	49555.21	0.0008

CONCLUSION

In conclusion, based on the experimental results, the GPR radargram showed a hyperbolic signature, indicating reflection from the rebar in the reinforced concrete beam, whereas the SFRC sample showed a hazy image, like radio static, with multiple overlapping hyperbolas. The hazy image may represent the uniformity of steel fibre in the SFRC beam. The radargram hazy image is heavier and more sophisticated for a 1.5% steel fibre fraction volume than for a 0.5% steel fibre fraction volume, showing the least.

The results of compressive strength for cube sample and broken beam sample show the same trend of increment in compressive strength for 0.5% steel fibre fraction volume, which for 7, 14, and 28 days are 137.1 N/mm^2, 133.7 N/mm^2, and 181.2 N/mm^2 compared with 1.5% steel fibre fraction volume, which for 7, 14, and 28 days are 74.3 N/mm^2, 127.1 N/mm^2, and 88.1 N/mm^2. Steel fibre fraction volumes of 1.0% and 1.5% can be used to determine the best value for the 0.5% steel fibre fraction volume in terms of strength. In terms of flexural strength, the SFRC exhibits an increase in flexural strength as the volume fraction of steel fibre increases. Based on three distinct case studies, 1.5% steel fibre volume fraction exhibits the most flexural strength on day 28 of any other SFRC sample, whereas 0.5% steel fibre volume fraction exhibits the least. The results indicate that a 1.5% steel fibre volume fraction in SFRC yields the highest flexural strength, followed by 0.5% and 1.0%.

The correlation between compressive strength obtained from the rebound hammer test, cube compressive test, broken beam test, and four-point bending (4PB) flexural strength was successfully analysed using Regression-Based Analysis in NCSS 2021. ANOVA results show that the linear model with sum of squares values of 514870.8 and 9342.8,

and F-ratios of 2.5831 and 30.3762, indicates that the model is significant for compressive cube beam strength and flexural strength. However, the linear model's performance in converting compressive strength to rebound number (RN) is less significant, with an F-ratio of 0.0008 and a sum of squares of 49555.21. The significance levels of the t-test for compressive strength cube beams, flexural strength, and compressive strength RN were 0.1173, 0.1063, and 0.9771, respectively. The hypothesis that the slope is zero is not rejected because the t-test value exceeds 0.0500. The model has fitted the experimental data using the empirical correlation equation model obtained for the compressive strength of cubes and broken beams, flexural strength, and the compressive strength RN conversion for the SFRC beam, as presented in equations 1, 2, and 3.

ACKNOWLEDGEMENT

The authors would like to acknowledge the financial support for this study from the Ministry of Higher Education - Fundamental Research Grant Scheme of 600-IRMI/FRGS 5/3 (178/2019) and other supports from the Institute for Infrastructure Engineering and Sustainable Management (IIESM) and the Faculty of Civil Engineering, Universiti Teknologi MARA (UiTM) Shah Alam, Selangor, Malaysia. These supports are gratefully acknowledged.

REFERENCES

Al-Ameeri, A. (2013). The effect of steel fibre on some mechanical properties of self-compacting concrete. *American Journal of Civil Engineering, 1*(3), 102-110. https://doi.org/10.11648/j.ajce.20130103.14

Bachiri, T., Khamlichi, A., & Bezzazi, M. (2018). Bridge deck condition assessment by using GPR: A review. *MATEC Web of Conferences, 191*, Article 00004. https://doi.org/10.1051/matecconf/201819100004

Briones-Bitar, J., Carrión-Mero, P., Montalván-Burbano, N., & Morante-Carballo, F. (2020). Rockfall research: A bibliometric analysis and future trends. *Geosciences, 10*(10), Article 403. https://doi.org/10.3390/geosciences10100403

Dinh, K., Zayed, T., & Tarussov, A. (2013). GPR image analysis for corrosion mapping in concrete slabs. In *Proceedings of the Annual Conference of the Canadian Society for Civil Engineering* (Vol. 3, pp. 2131–2140). Canadian Society for Civil Engineering.

Gehrig, M. D., Morris, D. V., & Bryant, J. T. (2004). *Ground penetrating radar for concrete evaluation studies* [Technical presentation paper]. Foundation Performance Association.

George, M., & Erdogmus, E. (2009, November). *Use of ground penetrating radar for construction quality assurance of concrete pavement*.

Giannopoulos, A. (2005). Modelling ground penetrating radar by GprMax. *Construction and Building Materials, 19*(10), 755-762. https://doi.org/10.1016/j.conbuildmat.2005.06.007

Harle, S. M. (2019). Experimental investigation on steel fibres in the concrete. *International Journal of Scientific Research in Network Security and Communication, 7*(4), 1-7.

Hasan, M. I., & Yazdani, N. (2016). An experimental and numerical study on embedded rebar diameter in concrete using ground penetrating radar. *Chinese Journal of Engineering, 2016*, Article 9714381. https://doi.org/10.1155/2016/9714381

He, X., Zhu, Z., Lu, G., & Lu, Q. (2009). Bridge management with GPR. In *2009 International Conference on Information Management, Innovation Management and Industrial Engineering* (Vol. 3, pp. 329-332). IEEE. https://doi.org/10.1109/ICIII.2009.387

Hintze, J. L. (2007). *NCSS user's guide I: NCSS statistical system*. NCSS.

Jhatial, A. A., Sohu, S., Bhatti, N. K., Lakhiar, M. T., & Oad, R. (2018). Effect of steel fibres on the compressive and flexural strength of concrete. *International Journal of Advanced and Applied Sciences, 5*(10), 16-21. https://doi.org/10.21833/ijaas.2018.10.003

Kumar Athithan, A. K., Robert Singh, R., & Sri Gomathi, A. B. (2017). Experimental study on steel fibre reinforced concrete in beam-column joint. *International Journal of Civil Engineering and Technology, 8*(8), 599-608.

Lakshmi, K. A., Sangoju, B., Vasanthakumar, & Rahamath, A. (2016). Estimation of rebar radius using ground penetrating radar. *International Journal of Emerging Technology in Computer Science & Electronics, 22*(2), 320-325.

Leucci, G. (2012). Ground penetrating radar: An application to estimate volumetric water content and reinforced bar diameter in concrete structures. *Journal of Advanced Concrete Technology, 10*(12), 411-422. https://doi.org/10.3151/jact.10.411

Liu, H., Lin, C., Cui, J., Fan, L., Xie, X., & Spencer, B. F. (2020). Detection and localization of rebar in concrete by deep learning using ground penetrating radar. *Automation in Construction, 118*, Article 103279. https://doi.org/10.1016/j.autcon.2020.103279

Morcous, G., & Erdogmus, E. (2009). *Use of ground penetrating radar for construction quality assurance of concrete pavement* (Report No. SPR-P1(08) P307). Mid-America Transportation Center, University of Nebraska-Lincoln. https://rosap.ntl.bts.gov/view/dot/24741

Neville, A. M. (2012). *Properties of concrete* (5th ed.). Pearson Education.

Profillidis, V. A., & Botzoris, G. N. (2019). Statistical methods for transport demand modeling. In *Modeling of transport demand* (pp. 163-224). Elsevier. https://doi.org/10.1016/B978-0-12-811513-8.00005-4

Rathod, H., Debeck, S., Gupta, R., & Chow, B. (2019). Applicability of GPR and a rebar detector to obtain rebar information of existing concrete structures. *Case Studies in Construction Materials, 11*, Article e00240. https://doi.org/10.1016/j.cscm.2019.e00240

Razak, N. A., Senin, S. F., & Hamid, R. (2015). Detection of sizes and locations air voids in reinforced concrete slab using ground penetrating radar and impact-echo methods. *Jurnal Teknologi, 74*(3), 63-67. https://doi.org/10.11113/jt.v74.4553

Shamsudin, A. M., Senin, S. F., Hamid, R., & Yusuf, K. (2015). Concrete delaminations location and its severity detection by visual inspection and ground penetrating radar. *Journal of Engineering Science and Technology, 10*(Special Issue on 4th International Technical Conference 2014), 1-12.

Shetty, M. S. (2005). *Concrete technology: Theory and practice* (Multicolour illustrative rev. ed.). S. Chand & Company.

Sultan, A. A., Mashrei, M. A., & Washer, G. A. (2020). Utilisation of Wilcoxon–Mann–Whitney statistics in assessing the reliability of non-destructive evaluation technologies. *Structures, 27*, 780-787. https://doi.org/10.1016/j.istruc.2020.06.024

Sun, H., Pashoutani, S., & Zhu, J. (2018). Nondestructive evaluation of concrete bridge decks with automated acoustic scanning system and ground penetrating radar. *Sensors, 18*(6), Article 1955. https://doi.org/10.3390/s18061955

Van Eck, N. J., & Waltman, L. (2020). *VOSviewer manual* (Version 1.6.16). Universiteit Leiden, Centre for Science and Technology Studies. https://www.vosviewer.com/documentation/Manual_VOSviewer_1.6.16.pdf

Warren, C., & Giannopoulos, A. (2016). Experimental and modelled performance of a ground penetrating radar antenna in lossy dielectrics. *IEEE Journal of Selected Topics in Applied Earth Observations and Remote Sensing, 9*(1), 29-36. https://doi.org/10.1109/JSTARS.2015.2430933

Wiwatrojanagul, P., Sahamitmongkol, R., & Tangtermsirikul, S. (2018). A method to detect lap splice in reinforced concrete using a combination of covermeter and GPR. *Construction and Building Materials, 173*, 481-494. https://doi.org/10.1016/j.conbuildmat.2018.04.027

Zaki, A., Megat Johari, M. A., Wan Hussin, W. M. A., & Jusman, Y. (2018). Experimental assessment of rebar corrosion in concrete slab using ground penetrating radar (GPR). *International Journal of Corrosion, 2018*, Article 5389829. https://doi.org/10.1155/2018/5389829

Zhou, F., Chen, Z., Liu, H., Cui, J., Spencer, B. F., & Fang, G. (2018). Simultaneous estimation of rebar diameter and cover thickness by a GPR-EMI dual sensor. *Sensors, 18*(9), Article 2969. https://doi.org/10.3390/s18092969